Neurophotonics

Neurophotonics.SPIEDigitalLibrary.org

Cortical responses to shape-from-motion stimuli in the infant

Amy Hirshkowitz
Marisa Biondi
Teresa Wilcox

SPIE.

Amy Hirshkowitz, Marisa Biondi, Teresa Wilcox, "Cortical responses to shape-from-motion stimuli in the infant," *Neurophoton.* **5**(1), 011014 (2017), doi: 10.1117/1.NPh.5.1.011014.

Neurophotonics 5(1), 011014 (Jan–Mar 2018)

Cortical responses to shape-from-motion stimuli in the infant

Amy Hirshkowitz,[a] Marisa Biondi,[b] and Teresa Wilcox[b,*]
[a]Baylor College of Medicine, Clinical Care Center, Houston, Texas, United States
[b]Texas A&M University, Department of Psychology, College Station, Texas, United States

Abstract. Our ability to extract three-dimensional (3-D) object structure from motion-carried information is a basic visual capacity that is fundamental to object perception. Despite a rich body of behavioral work demonstrating that infants are sensitive to motion-carried information from the early months of life, little is known about the cortical networks that support infants' use of motion-carried information to extract 3-D object structure. This study assessed patterns of cortical activation in infants aged 4 to 6 months as they viewed two types of visual stimuli: (a) shape-from-motion (SFM) displays, where coherent motion of randomly distributed dots gave rise to the percept of 3-D shape and (b) random motion (RM) displays, where dots' motions lacked a coherent structure and gave rise to the percept of randomly moving dots. Functional near-infrared spectroscopy was used to assess activation in occipital, inferior parietal, and posterior temporal cortex. The optical imaging data revealed differential responding to SFM and RM in lower level object processing areas than typically observed in the adult. Possible explanations for this pattern of results are considered.
[DOI: 10.1117/1.NPh.5.1.011014]

Keywords: infants; shape-from-motion; functional near-infrared spectroscopy; occipital cortex; parietal cortex; temporal cortex.

Paper 17046SSRR received Apr. 1, 2017; accepted for publication Sep. 1, 2017; published online Oct. 11, 2017.

1 Introduction

Our perception of three-dimensional (3-D) objects is determined by a complex set of visual processes in which two-dimensional (2-D) retinal input is transposed into 3-D images. The depth structure of 3-D objects can be extracted from a variety of visual cues that can be roughly categorized as motion-carried, binocular disparity, and pictorial. Of these three, motion-carried information is the first to emerge in infancy and is fundamental to visual perception throughout the life span. There is a rich history of research demonstrating that infants draw on motion-carried, or kinetic, information to extract spatial layout, parse surfaces, and form unified representations of objects when visual information is limited. For example, infants 2 to 4 months of age use accretion and deletion of texture and boundary flow to segregate textured surfaces in the depth plane,[1] the relative motion of grouped elements against a static background to parse surface area into components,[2,3] and common motion of visible surfaces to complete partially occluded objects.[4,5] There is also evidence that infants draw on motion-carried information to extract the 3-D structure of whole objects. For example, infants use information gained through optic flow to extract object form and can recognize that form from a unique perspective.[6–10] What has yet to be identified are the cortical structures that support these early emerging capacities. The current study focuses on cortical areas that support infants' use of motion-carried information to extract 3-D object structure.

1.1 *Processing of Shape-from-Motion in Infants: Behavioral Studies*

Initial studies investigating infants' capacity to extract 3-D structure from motion-carried information used displays containing objects 3-D in nature. For example, infants aged 4 months were habituated to a videotape or projected shadow of a 3-D object continuously moving, on alternating trials, around two different rotational axes.[4,11] In test trials, infants were presented with the same object and a different object, on alternating trials, moving around a third (new) rotational axis. Infants looked longer at the unfamiliar than the familiar object, suggesting that they had extracted the 3-D structure of the object seen in habituation trials and recognized it as structurally distinct from the unfamiliar test objects. Additional studies confirmed that kinetic information is critical to the extraction of 3-D form; infants do not extract 3-D structure from successive static images.[4,11] Also, infants extract 3-D structure independent of binocular disparity information; infants successfully extract 3-D structure under monocular viewing conditions.[10,12]

One limitation of using 3-D displays containing real objects or 2-D depictions of 3-D objects, however, is that they contain information about contour and intersection of lines. Figural information about shape is embedded in the stimuli, limiting conclusions that one can draw about infants' use of motion-carried information, alone. To control for this possibility, subsequent studies employed random-dot stimuli, which are created when randomly distributed dots are projected onto the surfaces of a simple geometric shape (e.g., cube or cylinder) that rotates around a 3-D axis. It is the coherent structure of the dots' motion that gives rise to the percept of a 3-D shape, often referred to as shape-from-motion (SFM). When the dots' motions lack a coherent structure, the percept is one of randomly moving dots or random motion (RM). Research conducted with adult participants indicates that the mature visual system readily extracts a percept of 3-D structure from SFM displays relatively early in the visual processing stream under a variety of

*Address all correspondence to: Teresa Wilcox, E-mail: twilcox@tamu.edu

2329-423X/2017/$25.00 © 2017 SPIE

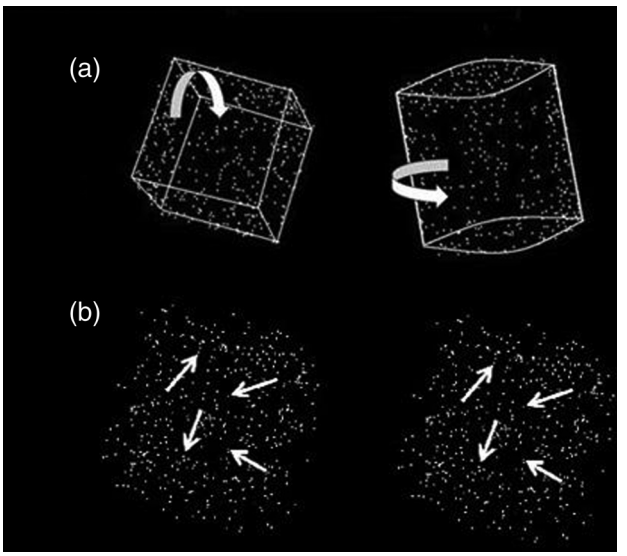

Fig. 1 The stimuli used in the current experiment, similar to those from Hirshkowitz and Wilcox (2013): (a) SFM cube and cylinder, respectively, and (b) RM cube and cylinder, respectively. White outlines and arrows in the SFM stimuli illustrate perceived contour and motion but were not present in the display. White arrows in the RM stimuli illustrate direction of motion but were not present in the display. Video of an SFM cube undergoing a 135-deg rotation (Video 1, MPEG, 845 KB [URL: http://dx.doi.org/10.1117/1.NPh.5.1.011014.1]) and the corresponding RM cube display (Video 2, MPEG, 772 KB [URL: http://dx.doi.org/10.1117/1.NPh.5.1.011014.2]).

conditions.[13–15] Using displays similar to those designed for adults, Hirshkowitz and Wilcox (2013) investigated 3- to 5-month-old and 8- to 9-month-old infants' ability to extract 3-D structure in random-dot displays. In these studies, infants were first presented with familiarization trials composed of SFM and RM displays (Fig. 1) seen on alternating trials. In the SFM display, coherent motion of the dots specified a 3-D form (e.g., a cube). In the RM display, the motion of the dots was randomly distributed—that is, the dots moved at the same velocity as in the SFM display but the direction of the dots' motion was randomly assigned. Following familiarization trials, infants were presented with test trials, in which the familiar SFM display (e.g., cube) was paired with a SFM display (e.g., cylinder). Visual attention to the familiarization and test displays was measured using a remote eye tracker. The results indicated that both age groups spent significantly more time fixating on the unfamiliar than familiar SFM display in the test trials, revealing that infants successfully extracted shape from the coherent motion displays. This is the first direct evidence that infants, like adults, extract 3-D object structure from coherent motion displays. What might be the underlying cortical basis of this early developing capacity?

1.2 *Cortical Basis of Shape-from-Motion Processing in the Adult Brain*

There is a considerable body of research on the neural basis of motion and shape processing in the human adult. It is well known that area MT+/V5 (Fig. 2) mediates the perception and analysis of motion-carried information. Most relevant to the current research is that MT+/V5 responds to motion in visual stimuli, regardless of whether motion is coherent or incoherent.

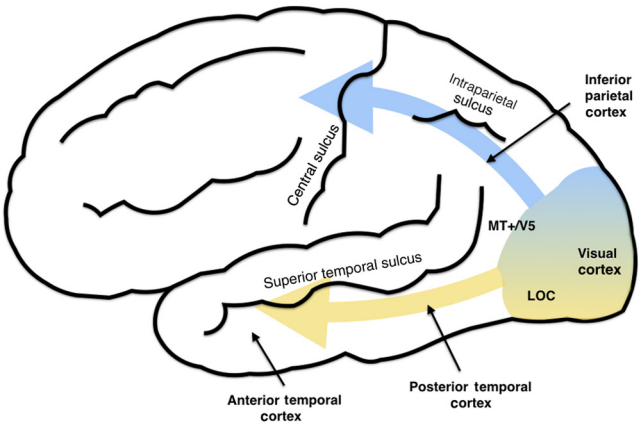

Fig. 2 Lateral view of the adult human brain with major sulci labeled. Dorsal and ventral streams are indicated with blue and yellow highlighted arrows, respectively. The approximate locations of MT+/V5 and LOC, as well as inferior parietal cortex and posterior temporal cortex, are indicated.

However, there is evidence that more robust responses are obtained in MT+/V5 with greater coherence.[16–19] For example, Rees et al. (2000) reported that the blood-oxygen-level dependent (BOLD) response in MT+/V5 increased with increasing global coherence. In these studies, the percentage of dots moving coherently on a 2-D surface was 0%, 6.25%, 12.5%, 25%, 50%, or 100%. Displays containing randomly placed static dots[20,21] or random patterns of flickering dots[22] do not elicit activation in MT+/V5, revealing the motion specificity of MT+/V5 responses. Finally, some researchers have reported that when greater activation to coherent than RM is observed in MT+/V5, it is right lateralized.[17,23]

When motion-carried information is coherent and gives rise to the percept of shape, occipital–temporal areas are also activated. It is important to note, however, that MT+/V5 and occipital–temporal areas are engaged for different reasons. While activation in MT+/V5 is driven by motion of the retinal image,[24] activation in occipital–temporal areas, which typically include the lateral occipital complex (LOC), is driven by the percept of shape.[22,25–28] There is also evidence that the area between LOC and MT+/V5 responds to moving shapes.[27,29,30] That is, while MT+/V5 responds selectively to motion (whether or not motion gives rise to a shape percept) and LOC responds selectively to shape (regardless of whether shape is specified by static contour or motion cues), there is an area between MT+/V5 and LOC that responds to moving shapes.

Coherent motion stimuli also elicit activation in inferior parietal cortex (Fig. 2). More specifically, activation has been observed near the occipital–parietal border in response to SFM stimuli but not to RM or static dot stimuli.[18,20,21,23] Inferior parietal areas appear to be sensitive to shape information regardless of the type of information (e.g., motion-carried information, contour, or disparity depth cues) that gave rise to the percept of shape.[14,18,20,23,31,32]

In sum, there is now considerable evidence that both ventral and dorsal areas contribute to the percept form from coherent patterns of motion in random dot displays.[23,32–34] One hypothesis is that 3-D shape perception depends on the integration of global motion processing, which is mediated by dorsal areas and shape recognition processing, which is mediated by ventral areas.[34]

Despite the importance of motion-carried information to object perception and a wealth of information about the cortical areas that support SFM processing in the adult, we have no information about the functional development of these cortical areas in the human infant. The goal of the current research is to fill this gap in knowledge by investigating cortical responses in occipital, temporal, and parietal regions to SFM and RM stimuli in young infants. One might predict that basic visual processes that draw on motion-carried information, which is fundamental to object perception from the early months of life, would be mediated by similar cortical areas in the infant and adult brain. However, there is reason to question this hypothesis. Neuroimaging studies conducted with infant macaque monkeys have reported that global motion and form processing are more likely to activate primary visual cortex (V1 or V4) than extra striate cortex (MT+/V5).[35,36] In mature macaque monkeys, greater activation is obtained in extra striate than primary visual cortex to the same global motion and form displays (similar to the findings obtained in adult humans). The outcome of the current study will provide insight into the extent to which the human brain is functionally specialized for SFM stimuli in the early months of life and the area(s) of the cortex in which this specialization is observed.

1.3 *Current Research*

Infants aged 4 to 6 months were presented with SFM and RM stimuli similar to those of Hirshkowitz and Wilcox (2013). Functional near-infrared spectroscopy (fNIRS) was used to assess changes in cortical activation, relative to a baseline stimulus (static, flickering dots), in response to the SFM and RM stimuli. Optodes were placed over occipital–temporal–parietal areas known to respond selectively during motion and object processing in adults. If motion and object processing areas in the infant brain are organized similar to those of the adult, we would expect to obtain activation to SFM and RM in cortical areas near MT+/V5. In contrast, we would expect to obtain activation to SFM but not RM stimuli in occipital–temporal areas in the ventral stream and inferior parietal areas in the dorsal stream. Alternatively, if the areas of the cortex that process motion and form in the human infant brain are organized similar to that of the infant macaque, we would expect to see differential responses to SFM and RM in lower level visual cortex rather than extra striate (higher level) cortex.

2 Experiment

2.1 *Methods*

2.1.1 *Participants*

Participants were 14 healthy full-term infants aged 4 to 6 months (6 males; range 4 months 2 days to 6 months 23 days; M age = 161 days). Parents reported their infant's ethnicity/race as Caucasian ($n = 11$) or Hispanic ($n = 3$). Fifteen additional infants were tested but eliminated from the final sample because of difficulty obtaining an optical signal ($n = 11$), procedural error ($n = 3$), or crying ($n = 2$). Although this number is higher than preferred and higher than our lab typically reports, it is within the range observed in infant fNIRS studies.[37] One reason for the high attrition rate in the current experiment is that the headgear covered cortical areas from which it is particularly difficult to measure. The skull overlying occipital–temporal–parietal areas has a significant amount of curvature, along horizontal and vertical planes; it is challenging to get optodes to lay firmly along this curved surface. Parents were offered $5 or a lab T-shirt for participation. This experiment was carried out in accordance with the recommendations and approval (IRB2004-0140D) of the Institutional Review Board, Division of Research, Texas A&M University with written informed consent from the parents/guardians of all infant participants. All parents/guardians gave written informed consent in accordance with the Declaration of Helsinki.

2.1.2 *Apparatus and data recording*

A remote eye tracker (Tobii T60 XL) was used to measure eye movements during stimuli presentation. The infrared corneal reflection eye tracker was embedded in the lower portion of a 24 in flat screen monitor set to a resolution of 1024×768 pixels. It detected the position of the pupil and the corneal reflection of the infrared light from both eyes. The Tobii T60 XL records data at 60 Hz with an average accuracy of 0.5 deg visual angle and a head movement compensation drift of G0.1. Fixation data were defined using the Tobii fixation filter (version 2.2.8) with a velocity threshold of 35 pixels and a distance threshold of 35 pixels. The total duration of looking during each test trial was calculated by the fixation data sums for each trial. The monitor was mounted on an adjustable arm so that it could be positioned optimally for each infant. A full-face view of the infant was recorded by a Logitech Webcam Pro 9000 positioned atop the monitor during stimuli presentation. Tobii Studio was used to present the stimuli on a Dell Precision M6400 desktop computer with a Windows XP operating system.

One might be concerned that the wavelength of light emitted by the Tobii eye tracker would interfere with the fNIRS signal. Although Tobii does not publically release specific wavelength measurements for its eye-trackers, the light emitted is within the range of 600 to 900 nm. Hence, the wavelength of infrared light emitted by the eye tracker could potentially overlap with the wavelengths detected by our optical imaging device. We were aware of this potential problem when designing the experiment. We addressed this concern by comparing the fNIRS signal obtained when the eye tracker was off instead of when it was on. No significant change in the signal (off versus on) was observed. As an added precaution, however, once the headgear was placed on the infants head the optode arrays were covered with black, light-blocking material.

In addition to number of fixations (fixation count) and duration of looking, two other visual scanning measures were extracted. Both measures were computed using fixation coordinates (x, y) for each look within each trial. The first measure we calculated was the distance from one fixation coordinate to the next (in pixels); we call this distance. The second measure we calculated was the angle between one fixation coordinate and the next (in deg); we call this measure direction. We reasoned that if infants perceived the 3-D SFM shape, they would scan the moving contour of the shape in a systematic fashion, and this would be associated with HbO responses. In contrast, we predicted that viewing RM displays that do not possess moving contour would not elicit systematically distributed infant scanning. In short, we expected the distance and direction between looks to be smaller (i.e., directed at local contour rather than randomly distributed across the display) when infants viewed the SFM than RM displays.

2.1.3 *Stimuli and design*

The SFM and RM stimuli, displayed in Fig. 1, were similar to those of Hirshkowitz and Wilcox (2013) and adapted from Murray et al. (2004). The SFM displays were composed of 450 white dots (against a black background) orthographically projected onto the surfaces of a simple geometric shape (cube or cylinder) that rotated either 90 deg, 135 deg, or 180 deg around the 3-D *y*-axis during each 5-s trial. The RM displays were composed of the same number of dots moving at the same velocity except that the direction of each dots' motion was randomly assigned. The stimuli (SFM and RM) were 15 cm × 13 cm and presented at the center of the screen. To maintain infants' attention, each SFM and RM trial was accompanied by a nonverbal, nonmusical sound (e.g., whistle or whirring); sounds were counterbalanced across stimuli. All Infants viewed six pairs of SFM-RM trials (two SFM that each rotated 90 deg, 135 deg, or 180 deg around the 3-D axis), for a total of 12 trials. The order in which the SFM and RM displays were presented within each pair was counterbalanced across participants. Each SFM and RM display was preceded (and followed) by a 10-s display composed of a solid-colored screen that pulsed, with soft music playing in the background. This was used as the baseline display to maintain infants' attention. We chose not to use a static random-dot scrambled image or a pulsing static random-dot scrambled image to avoid potential dot-shape after effects.

2.1.4 *Procedure*

Infants were seated in a parent's lap 65 cm away from the monitor, in which the stimuli were presented. The testing room was dark and black curtains shielded the infant/parent from the rest of the testing room. Parents were instructed to close their eyes or wear blacked out glasses during the test session. To obtain reliable and valid eye movement data, the Tobii Studio infant calibration program was used prior to stimulus presentation. Animated stimuli were used to direct attention to five gaze positions covering over 80% of the viewing area.

2.1.5 *Functional near-infrared spectroscopy instrumentation*

The imaging equipment contained four fiber-optic cables that delivered near-infrared light to the scalp of the participant (emitters), eight fiber-optic cables that detected the diffusely reflected light at the scalp (detectors), and an electronic control box that served as the source of the near-infrared light and the receiver of the reflected light. The control box produced light at wavelengths of 690 nm, which is more sensitive to deoxygenated blood, and 830 nm, which is more sensitive to oxygenated blood, with two laser-emitting diodes (TechEn, Inc.). Laser power emitted from the end of the diode was 4 mW. Light was square wave modulated at audio frequencies of ∼4 to 12 kHz. Each laser had a unique frequency so that synchronous

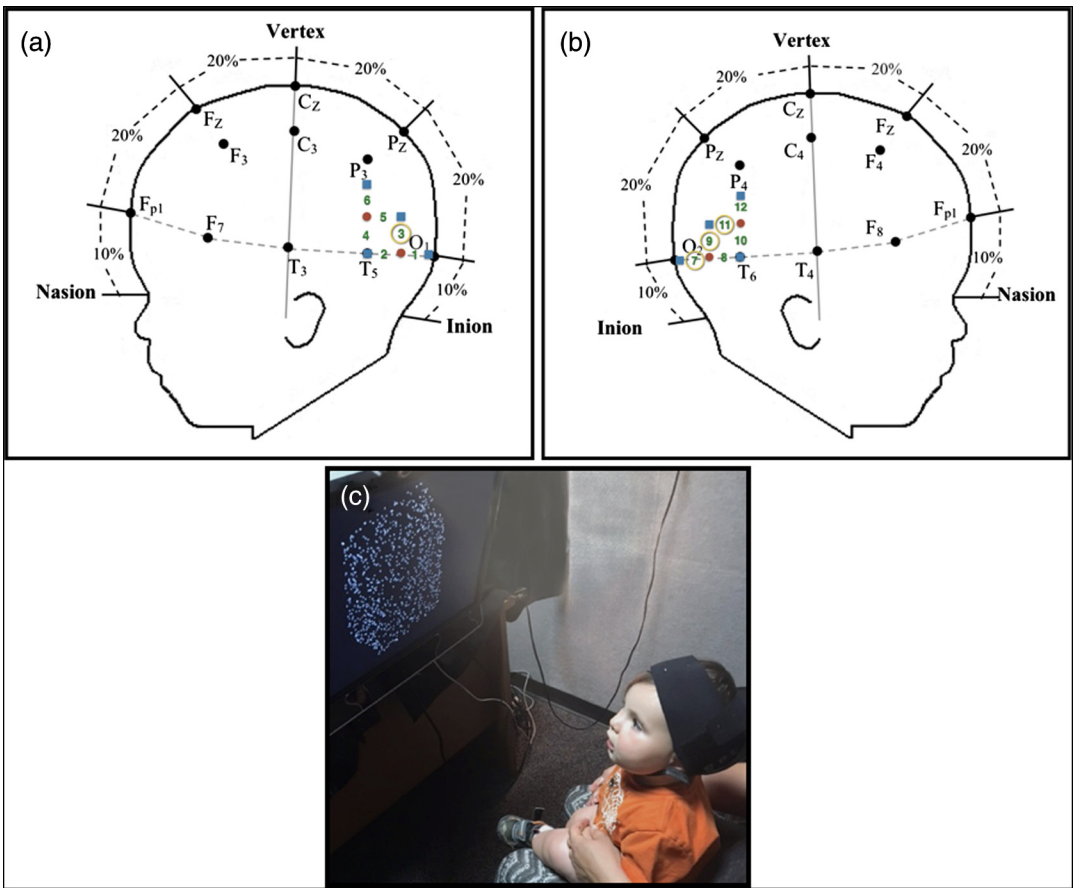

Fig. 3 Configuration of emitters (red circles) and detectors (black squares), and the six corresponding channels (numbered) from which optical signals were measured, in the (a) left and (b) right hemispheres. Approximate location of the emitters and detectors and corresponding channels are placed on a schematic of an infant's head relative to the 10–20 International EEG system. The circled channels are those from which a significant response to the SFM stimuli was obtained. (c) Infant participating in the study.

detection could uniquely identify each laser source from the photodetector signal. Ambient illumination from the testing room did not interfere with the laser signals because environmental light sources modulate at a different frequency. Each emitter delivered both wavelengths of light and each detector responded to both wavelengths. The signals received by the electronic control box were recorded and processed via data acquisition software developed by TechEn.

Prior to the experimental session, infants were fitted with a custom-made headgear that secured the fiber optics to the scalp. Configuration of the sources and detectors within the headgear, placement of the sources and detectors on the infant's head, and location of the corresponding channels are displayed in Fig. 3. The headgear was placed on the infant's head using O1 and O2 as primary anchors and T3 and T4 as secondary anchors. The headgear was designed to assess hemodynamic responses in dorsal and ventral object processing areas. On the basis of currently available cortical maps for infants[38,39] and adults,[40] we extrapolated that channels 3/9 and 5/11 measured from middle/upper occipital gyrus, including MT+/V5; that channels 1/7 and 2/8 measured from occipital–temporal areas, including LOC; that channels 4/10 channels measured from posterior temporal cortex; and that channels 6/12 measured from inferior parietal cortex. Source–detector separation was 2 cm. The headgear was not elastic so the distance between sources and detectors on each side of the head remained fixed. The mean head circumference of infants was 42.9 cm (SD = 1.4 cm). We also measured the distance between infants' nasion and inion (N-I) ($M = 24.7$ cm, SD = 2.7 cm) and between internal auditory canals (IAC–IAC) over the top of the head ($M = 24.9$ cm, SD = 3.1 cm).

2.1.6 *Processing of functional near-infrared spectroscopy data*

The fNIRS test data were processed, for each channel and event condition separately, using Homer2. The raw signals were acquired at the rate of 50 samples per second, converted to relative concentrations of oxygenated (HbO) and deoxygenated (HbR) blood using the modified Beer–Lambert law. The optical signals were digitally low-pass filtered at 0.50 Hz and high-pass filtered at 0.010 Hz, and a principal components analysis (PCA) was performed to remove systemic physiology common across channels (accounting for up to 80% of the variance). A recursive motion correction procedure[41] was implemented to objectively identify and replace (if possible) channel specific motion artifacts. A motion artifact was defined as a change in the absolute signal amplitude of greater than 0.5 units over 0.5 s (using a mask of 1 s). A targeted PCA filter removed up to 97% of the variance in the signal due to motion, with a maximum of five iterations for correction. For each test trial, changes in HbO and HbR were examined relative to the 2-s prior to the onset of the test event (i.e., the mean optical signal from −2 to 0 was set to 0 and this was used as the baseline). Of the 84 possible SFM and 84 possible RM trials (14 infants × 6 trials for each condition), infants completed 72 SFM and 78 RM trials. The mean number of trials completed in the SFM condition ($M = 4.86$, SD = 1.29) and the RM condition ($M = 5.14$, SD = 0.95) did not differ significantly ($t = 1.30$, $df = 13$, $p = 0.218$).

2.2 *Results*

2.2.1 *Preliminary analyses*

Preliminary analysis of the eye tracking (mean duration of looking and fixation count) and optical imaging data revealed no significant effects, or interactions, involving sex. Hence, this factor will not be included in the main analyses. However, given the relatively small number of males and females tested, null effects should be interpreted with caution.

2.2.2 *Eye tracking data*

The number of times infants fixated to the test stimuli was averaged over trials and infants for each event condition separately. Paired-sample t-tests indicated that fixation counts to the SFM ($M = 0.83$, SD = 0.36) and the RM ($M = 0.92$, SD = 0.37) stimuli did not differ significantly ($t = -1.40$, $df = 13$, and $p = 0.19$). Infants' duration of looking to the SFM and RM stimuli was also averaged, separately, over trials and infants. Paired-sample t-tests indicated that duration of looking to the SFM ($M = 2.12$, SD = 1.70) and the RM ($M = 2.12$, SD = 1.70) stimuli did not differ significantly ($t < 1$, $df = 13$). Together, these data suggest that the infants spent about the same amount of time attending to the SFM and the RM stimuli. Hence, differences in hemodynamic responses to SFM and RM stimuli cannot be attributed to attention factors.

Infants' mean distance and direction between looks (averaged over trials and infants for each event condition, separately) were analyzed in the same manner as mean fixation and duration

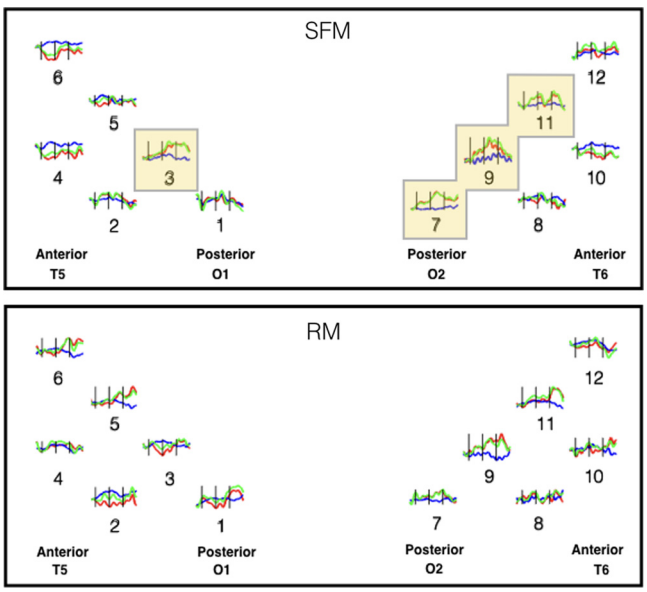

Fig. 4 Mean hemodynamic responses in the left and right hemisphere to the SFM and RM stimuli. O1/O2 and T5/T6 correspond to the International 10–20 coordinates shown in Figs. 3(a) and 3(b). The red curves indicate change in oxyhemoglobin concentration (HbO), the blue curves indicate change in deoxyhemoglobin concentration (HbR), and the green curves indicate the sum total of HbO and HbR (HbT). The black vertical lines indicate time points 0, 5, and 15 s, respectively, (0 and 5 s correspond with the onset and offset of the stimulus). The horizontal axis indicates time (−2 to 20 s) and the vertical axis indicates change in optical density units (ΔOD, in μM cm). The numbers under each waveform indicate the channel from which the data were obtained. The highlighted channels indicate the channels from which a significant HbO response was obtained.

of looking. Paired-sample *t*-tests indicated that distance of looks (in pixels) to the SFM ($M = 179.58$, SD $= 89.38$) and the RM ($M = 210.78$, SD $= 67.03$) stimuli did not differ significantly ($t = -1.25$, $df = 13$, $p = 0.23$). Paired-sample *t*-tests indicated that direction of looking (in degree of angle) to the SFM ($M = 44.60$, SD $= 7.14$) and the RM ($M = 44.08$, SD $= 10.66$) stimuli did not differ significantly ($t = 1.31$, $df = 13$, $p = 0.21$).

Table 1 Mean and (standard deviation) HbO responses to the SFM and RM stimuli, for each channel. *T* and *p* values (one-tailed) are reported for each channel. BFs are also reported for each channel. Those channels, in which the *t*-test effect was significant ($p < 0.05$), are highlighted with grayscale. Cohen's *d* are reported for channels, in which a response was obtained in the predicted direction.

	SFM					
HBO	*M* (SD)	*t*-value	*df*	*p*-value	Cohen's *d*	BF
			Left hemisphere			
Channel 1	0.2048 (0.6691)	1.145	13	0.137	0.306	0.795
Channel 2	0.0496 (0.9199)	0.202	13	0.422	0.054	0.315
Channel 3	0.6748 (1.1128)	2.269	13	0.021	0.606	3.573
Channel 4	−0.2476 (0.8545)	−1.084	13			0.146
Channel 5	−0.0473 (1.1237)	−0.158	13			0.241
Channel 6	−0.2167 (1.1509)	−0.705	13			0.174
			Right hemisphere			
Channel 7	0.5407 (0.9164)	2.208	13	0.023	0.590	3.264
Channel 8	0.1493 (0.6544)	0.757	10	0.234	0.228	0.569
Channel 9	0.6658 (1.1096)	2.245	13	0.022	0.600	3.449
Channel 10	−0.3452 (0.6918)	−1.655	10			0.135
Channel 11	0.2528 (0.4186)	2.260	13	0.021	0.604	3.526
Channel 12	0.1587 (0.9218)	0.644	13	0.266	0.172	0.467
HBO			RM			
			Left hemisphere			
Channel 1	0.1317 (0.6884)	0.713	13	0.244	0.191	0.501
Channel 2	−0.0996 (0.5467)	−0.682	13			
Channel 3	−0.0903 (0.7518)	−0.449	13			
Channel 4	0.0958 (1.0046)	0.357	13	0.364	0.095	0.359
Channel 5	0.2861 (1.4973)	0.715	13	0.244	0.191	0.500
Channel 6	0.2391 (0.8445)	1.059	13	0.155	0.283	0.721
			Right hemisphere			
Channel 7	0.1810 (0.7804)	0.868	13	0.201	0.232	0.586
Channel 8	−0.0268 (0.8694)	−0.115	13			
Channel 9	0.2887 (0.6316)	1.711	13	0.056	0.457	1.617
Channel 10	0.0054 (0.7829)	0.025	12	0.491	0.007	0.283
Channel 11	0.1090 (0.7239)	0.563	13	0.292	0.150	0.432
Channel 12	−0.1241 (0.7692)	−0.604	13			

2.2.3 *Optical imaging data*

Hemodynamic response curves for each condition and channel are presented in Fig. 4. For each of the 12 channels (6 channels within each hemisphere), hemodynamic responses were averaged over 5 to 10 s. This interval was chosen because pilot data suggested that hemodynamic responses to the SFM and RM stimuli are well initiated by 5-s poststimulus and return to baseline by 15-s poststimulus. Responses were then averaged over trial and infant, for each of the two event conditions, separately. Mean hemodynamic responses are reported in Table 1 (HbO) and Table 2 (HbR). However, because HbO responses are typically more robust than HbR responses,[42] we focus our analyses on HbO.

Data were analyzed in two steps. First, relative changes in mean HbO for each condition and channel were compared to 0 using *t*-tests (Table 1). We had a directional hypothesis (changes in HbO would be in the positive direction), hence one-tailed tests were used. In the left hemisphere, significant activation was obtained in channel 3. In the right hemisphere, significant activation was obtained in channels 7, 8, and 9. Cohen's *d* (see Table 1) indicates medium effect sizes associated with each statistically significant effect.

In addition to conducting *t*-tests, we conducted Bayesian analyses to examine the robustness of our results.[43] In these analyses, we assessed the extent to which the alternative hypothesis, an increase in HbO relative to 0 (the null hypothesis would be no increase in HbO relative to 0), was supported. Bayes factors (BFs) are reported in Table 1. A BF indicates that the data obtained are *B* times more likely under the alternative than null hypothesis. For example, a BF of 3 indicates that the data are 3 times more likely under the alternative hypothesis. A BF between 3 and 10 indicates substantial evidence for the alternative hypothesis. In all four channels, in which significant effects were obtained using *t*-tests, the BF was greater than 3. BFs equal to or greater than 3 were not obtained in any other channels.

In the second data analysis step, we assessed the extent to which the HbO responses obtained to the SFM and RM displays differed significantly from each other. Because the three right hemisphere channels that showed activation to SFM (but not RM) were spatially contiguous, we averaged the responses across those channels to create a right hemisphere region of interest (ROI).[37,44] T-tests revealed that in channel 3 a significantly greater response was obtained to the SFM than RM stimuli, $t = 2.53$, $df = 13$, $p = 0.0125$ (one-tailed), and Cohen's $d = 1.441$. In addition, the mean HbO response obtained in the right hemisphere ROI was significantly greater to the SFM stimuli ($M = 0.486$, SD $= 0.661$) than RM stimuli ($M = 0.193$, SD $= 0.530$), $t = 1.84$, $df = 13$, $p = 0.044$ (one-tailed), and Cohen's $d = 0.502$. Together, these results provide strong evidence that striate cortex, but not extra striate cortex, responds differentially to SFM than RM stimuli.

2.2.4 *Correlation between visual scanning and HbO responses*

To assess the extent to which visual scanning measures were associated with HbO responses to the SFM stimuli (we did not obtain HbO responses to the RM stimuli), we conducted correlational analyses between each of the four eye-tracking measures (fixation count, duration of looking, distance of looks, and direction of looks) and HbO responses in channel 3 and the right hemisphere ROI. The results of these analyses are reported in Table 3. Contrary to our expectations, none of the visual scanning measures was correlated with HbO responses to SFM stimuli in channel 3 or the right hemisphere ROI. Although we have previously reported no difference between SFM and RM for any of these visual scanning measures,[9] we thought it possible that these measures would be correlated with HbO responses. One interpretation of these data is that hemodynamic

Table 2 Mean and (standard deviation) HbR responses to the SFM and RM stimuli, for each channel.

HBR	SFM
Left hemisphere	*M* (SD)
Channel 1	0.0257 (0.3525)
Channel 2	−0.0100 (0.3459)
Channel 3	0.0353 (0.6291)
Channel 4	0.0526 (0.5141)
Channel 5	0.0415 (0.5537)
Channel 6	0.1958 (0.8288)
Right hemisphere	*M* (SD)
Channel 7	−0.0047 (0.5471)
Channel 8	0.0956 (0.4719)
Channel 9	0.1477 (0.7720)
Channel 10	0.1510 (0.2767)
Channel 11	0.0692 (0.5765)
Channel 12	0.1906 (0.4514)
RM	
Left hemisphere	*M* (SD)
Channel 1	0.2058 (0.5117)
Channel 2	0.1941 (0.2877)
Channel 3	0.1012 (0.3689)
Channel 4	0.0055 (0.4871)
Channel 5	0.0105 (0.5035)
Channel 6	−0.0839 (0.6138)
Right hemisphere	*M* (SD)
Channel 7	−0.1199 (0.4841)
Channel 8	0.1250 (0.4966)
Channel 9	−0.0022 (0.5500)
Channel 10	0.1827 (0.5680)
Channel 11	0.2200 (0.4223)
Channel 12	0.1027 (0.3922)

Table 3 Pearson correlations between the four visual scanning measures (duration of looking, fixation count, distance of looks, direction of looks) and HbO responses to the SFM stimuli obtained in channel 3 and in the right hemisphere ROI (channels 7, 9, and 11). Significance values are two-tailed.

	SFM			
	Duration of looking	Fixation count	Distance of looks	Direction of looks
	HbO channel 3			
Pearson correlation (r)	0.052	−0.192	−0.259	−0.129
Significance value (p)	0.859	0.512	0.371	0.659
N	14	14	14	14
	HbO right ROI			
Pearson correlation (r)	−0.191	−0.478	0.212	−0.165
Significance value (p)	0.514	0.084	0.467	0.572
N	14	14	14	14

responses are a more sensitive measure of SFM processing than behavioral measures.

3 Discussion

Behavioral studies have revealed that from the early months of life, human infants are sensitive to motion-carried information and extract 3-D form from coherent motion displays. The current research is the first to explore the cortical basis of this early developing capacity in young infants. The optical imaging data revealed robust HbO responses to SFM, but not RM, stimuli in striate areas. More specifically, in the right hemisphere, HbO responses were obtained in three spatially contiguous channels that measured primarily from middle/upper occipital gyrus. In the left hemisphere, one channel, also measuring from middle/upper occipital gyrus, showed a response to SFM but not RM stimuli. No HbO responses to the SFM nor RM stimuli were observed in extra striate areas.

One interpretation of these results, and the one to which we have already alluded, is that selective responding to SFM stimuli occurs in lower level visual object processing areas in the infant than the adult. This interpretation is consistent with data obtained with infant macaques, who are more likely to show cortical activation in V1/V4 than MT+/V5 during motion and form processing. In contrast, older macaques, like adult humans, are more likely to show activation in MT+/V5 than striate cortex under these experimental conditions.[35,36] An alternative interpretation is that the cortical activation observed in this study was in response to infants' processing of lower level visual features. The SFM and RM displayed were designed to contain the same number of dots moving at the same velocity. What differed was the extent to which the dots moved coherently. In the SFM, displays dots were projected onto the surfaces of the objects. The dots projected onto each surface moved in the same direction; each surface group moved in a different direction (this is what gave rise to the percept of a 3-D moving form). In contrast, in the RM displays, the direction of each dots' motion was randomly assigned; there were no groups of dots that moved together in the same direction. Hence, it is possible that in the SFM condition infants attended only to a subset of dots that moved in the same direction (if infants attended to all components, they would have the percept of 3-D form). We believe this unlikely for two reasons. First, there is a substantial body of behavioral data, obtained from different labs using different stimuli, demonstrating that infants as young as 2 months perceive form in SFM displays.[6–10] It would be highly unusual if infants in the present study did not extract 3-D form. Second, in order to obtain the perception of directional motion (but not 3-D form), infants must attend only to a small component of the display moving in the same direction. Although certainly not definitive, eye-tracking data suggest that directional scanning patterns did not differ significantly for the SFM and RM displays.

Unexpectedly, there were no areas from which we measured that responded to both the SFM and the RM stimuli. This may be due, in part, to the nature of the baseline stimuli. Remember that the baseline displays in the present experiments were solid-colored screens that pulsed, with soft music playing in the background. These displays, which served to maintain infants' attention during the baseline interval, did not contain motion yet were dynamic (contained energy). It is possible that if baseline displays had been composed of static dots, which contained no energy or motion, increased activation would have been obtained to both SFM and RM stimuli, while still obtaining greater activation to SFM than RM displays. In the adult, it is not uncommon to obtain increased BOLD responses to both SFM and RM stimuli in extrastriate areas, with greater responses to SFM than RM stimuli. In support of this hypothesis, there is evidence that infants show electrophysiological responses to coherent and random dot displays, as compared to static dot displays, in occipital areas. At the same time, responses to coherent and random dot displays differ from each other.[45] Additional fNIRS work is warranted to assess the extent to which extrastriate areas in the infant cortex are more sensitive to the distinction between coherent versus noncoherent motion than the distinction between displays that contain motion and those that do not contain motion.

Disclosures

No conflicts of interest, financial or otherwise, are declared by the authors.

Acknowledgments

We thank the staff of the Infant Cognition Lab at Texas A&M University for help with data collection and management, Dr. David A. Boas for designing the graphical user interface used to create the SFM and RM stimuli and for many helpful discussions about this project, and the infants and parents who so graciously participated in the research. This work was supported by NIH grant R01-HD057999 to TW. Data collection and manuscript preparation was supported by NIH grant R01-HD057999 to TW.

References

1. S. P. Johnson, "The development of visual surface perception: insights into the ontogeny of knowledge," in *Progress in Infancy Research*, C. Rovee-Collier, L. Lipsitt, and H. Hayne, Eds., Vol. **1**, pp. 113–154, Erlbaum, Mahwah, New Jersey (2000).
2. S. P. Johnson et al., "Development of perceptual completion originates in information acquisition," *Dev. Psychol.* **44**(5), 1214–1224 (2008).
3. S. P. Johnson and U. Mason, "Perception of kinetic illusory contours by 2-month-old infants," *Child Dev.* **73**, 22–34 (2002).
4. P. J. Kellman, "Perception of three-dimensional form by human infants," *Percept. Psychophys.* **36**(4), 353–358 (1984).
5. P. Kellman and E. Spelke, "Perception of partly occluded objects in infancy," *Cognit. Psychol.* **15**, 483–524 (1983).
6. M. E. Arterberry, L. G. Craton, and A. Yonas, "Infants' sensitivity to motion-carried information for depth and object properties," in *Visual Perception and Cognition in Infancy*, C. E. Granrud, Ed., pp. 215–234, Lawrence Erlbaum Associates, Inc., Hillsdale, New Jersey (1993).
7. M. E. Arterberry and A. Yonas, "Infant sensitivity to kinetic information for three-dimensional object shape," *Percept. Psychophys.* **44**(1), 1–6 (1988).
8. M. E. Arterberry and A. Yonas, "Perception of three-dimensional shape specified by optic flow by 8-week-old infants," *Percept. Psychophys.* **62**(3), 550–556 (2000).
9. A. Hirshkowitz and T. Wilcox, "Infants' ability to extract three-dimensional shape from coherent motion," *Infant Behav. Dev.* **36**(4), 863–872 (2013).
10. A. Yonas, M. E. Arterberry, and C. E. Granrud, "Four-month-old infants' sensitivity to binocular and kinetic information for three-dimensional-object shape," *Child Dev.* **58**(4), 910–917 (1987).
11. P. Kellman and K. Short, "Development of three-dimensional form perception," *J. Exp. Psychol.* **13**(4), 545–557 (1987).
12. C. Owsley, "The role of motion in infants' perception of solid shape," *Perception* **12**(6), 707–717 (1983).
13. L. Gilroy and R. Blake, "Physics embedded in visual perception of three-dimensional shape from motion," *Nat. Neurosci.* **7**(9), 921–922 (2004).
14. S. Murray, P. Schrater, and D. Kersten, "Perceptual grouping and the interactions between visual cortical areas," *Neural Networks* **17**, 695–705 (2004).
15. J. Tittle et al., "Systematic distortion of perceived three dimensional structure from motion and binocular stereopsis," *J. Exp. Psychol.* **21**(3), 663–678 (1995).
16. O. J. Braddick et al., "Brain areas sensitive to coherent motion," *Perception* **30**, 61–72 (2001).
17. G. Hesselmann, C. A. Kell, and A. Kleinschmidt, "Ongoing activity fluctuations in hMT+ bias the perception of coherent visual motion," *J. Neurosci.* **28**(53), 14481–14485 (2008).
18. S. Iwaki and J. W. Belliveau, "Neural interactions between dorsal and ventral visual subsystems while perceiving 3-D structure from 2-D motion," in *17th Int. Conf. on Biomagnetism Advances in Biomagnetism (BIOMAG, IFMBE Proc.)*, Vol. 28, pp. 286–289, Springer (2010).
19. G. Rees, K. Friston, and C. Koch, "A direct quantitative relationship between the functional properties of human and macaque V5," *Nat. Neurosci.* **3**, 716–723 (2000).
20. A. L. Paradis et al., "Visual perception of motion and 3-D structure from motion: an fMRI study," *Cereb. Cortex* **10**(8), 772–783 (2000).
21. W. Vanduffel et al., "Extracting 3D from motion: differences in human and monkey intraparietal cortex," *Science* **298**(5592), 413–415 (2002).
22. S. O. Murray, B. A. Olshausen, and D. L. Woods, "Processing shape, motion and three-dimensional shape-from-motion in the human cortex," *Cereb. Cortex* **13**(5), 508–516 (2003).
23. G. A. Orban et al., "Human cortical regions involved in extracting depth from motion," *Neuron* **24**, 929–940 (1999).
24. H. Kolster, R. Peeters, and G. A. Orban, "The retinotopic organization of the human middle temporal area MT/V5 and its cortical neighbors," *J. Neurosci.* **30**(29), 9801–9820 (2010).
25. K. Grill-Spector et al., "A sequence of object-processing stages revealed by fMRI in the human occipital lobe," *Hum. Brain Mapp.* **6**(4), 316–328 (1998).
26. K. Grill-Spector, Z. Kourtzi, and N. Kanwisher, "The lateral occipital complex and its role in object recognition," *Vision Res.* **41**(10–11), 1409–1422 (2001).
27. Z. Kourtzi et al., "Representation of the perceived 3-D object shape in the human lateral occipital complex," *Cereb. Cortex* **13**(9), 911–920 (2003).
28. P. Vachon et al., "Global motion stimuli and form-from-motion stimuli: common characteristics and differential activation patterns," *Int. J. Neurosci.* **119**(10), 1584–1601 (2009).
29. S. Ferber, G. K. Humphrey, and T. Vilis, "The lateral occipital complex subserves the perceptual persistence of motion-defined groupings," *Cereb. Cortex* **13**, 716–721 (2003).
30. Z. Kourtzi et al., "Object-selective response in the human motion area MT/MST," *Nat. Neurosci.* **5**(1), 17–18 (2002).
31. M. Kraut et al., "Object shape processing in the visual system evaluated using functional MRI," *Neurology* **48**, 1416–1420 (1997).
32. H. Peuskens et al., "Attention to 3-D shape, 3-D motion, and texture in 3-D structure from motion displays," *J. Cognitive Neurosci.* **16**(4), 665–682 (2004).
33. S. Iwaki, G. Bonmassar, and J. W. Belliveau, "Neuromagnetic brain responses during 3D object perception from 2D optic flow," *Int. Congr. Ser.* **1300**, 543–546 (2007).
34. S. Iwaki, G. Bonmassar, and J. W. Belliveau, "Dynamic cortical activity during the perception of three-dimensional object shape from two-dimensional random-dot motion," *J. Integr. Neurosci.* **12**(3), 355–367 (2013).
35. Z. Kourtzi et al., "Development of visually evoked cortical activity in infant macaque monkeys studied longitudinally with fMRI," *Magn. Reson. Imaging* **24**(4), 359–366 (2006).
36. C. Distler et al., "Functional development of the corticocortical pathway for motion analysis in the macaque monkey: a ^{14}C-2-deoxyglucose study," *Cereb. Cortex* **6**(2), 184–195 (1996).
37. S. Lloyd-Fox, A. Blasi, and C. E. Elwell, "Illuminating the developing brain: the past, present and future of functional near infrared spectroscopy," *Neurosci. Biobehav. Rev.* **34**(3), 269–284 (2010).
38. C. Kabdebon et al., "Anatomical correlations of the international 10–20 sensor placement system in infants," *NeuroImage* **99**, 342–356 (2014).
39. S. Lloyd-Fox et al., "Co-registering fNIRS with underlying cortical areas in infants," *Neurophotonics* **1**(2), 025006 (2014).
40. M. Okamoto et al., "Three-dimensional probabilistic anatomical cranio-cerebral correlation via the international 10–20 system oriented for transcranial functional brain mapping," *NeuroImage* **21**(1), 99–111 (2004).
41. M. A. Yücel et al., "Targeted principle component analysis: a new motion artifact correction approach for near-infrared spectroscopy," *J. Innovative Opt. Health Sci.* **7**(2), 1350066 (2014).
42. G. Strangman, M. A. Franceschini, and D. A. Boas, "Factors affecting the accuracy of near-infrared spectroscopy concentration calculations for focal changes in oxygenation parameters," *NeuroImage* **18**(4), 865–879 (2003).
43. J. K. Kruschke, *Doing Bayesian Data Analyses*, 2nd Ed., Elsevier, Amsterdam (2015).
44. M. Biondi, D. A. Boas, and T. Wilcox, "On the other hand: increased cortical activation to human versus mechanical hands in infants," *NeuroImage* **141**, 143–153 (2016).
45. A. L. H. van der Meer, G. Fallet, and F. R. van der Weel, "Perception of structured optic flow and random motion in infants and adults: a high-density EEG study," *Exp. Brain Res.* **186**(3), 493–502 (2008).

Biographies for the authors are not available.